

多树枝结构和立方结构 PbS 的水热合成及形成机理

王新军* 刘娟 柴春霞 李可 董玉涛 蒋凯*

(河南师范大学化学与环境科学学院, 新乡 453007)

摘要: 在无模板条件下, 用 $\text{Pb}(\text{NO}_3)_2$ 做铅源, $(\text{CH}_4\text{N}_2\text{S})$ 做硫源, 用水热法在 160 °C 反应 24 h 制备了结晶度好的多树枝结构 PbS。利用 XRD、SEM、EDX、TEM 对产物进行了表征, 结果表明所得产物为面心立方多树枝状结构, 单个树枝的长度为 1.0~3.0 μm 。此外, 在碱性条件下丙三醇/水体系中制备了具有不同凹面的立方结构 PbS, 边长为 2.0~5.0 μm 。对 2 种不同形态 PbS 的影响因素进行了讨论, 并提出了形成机理。同时对其荧光及紫外性质进行了研究, 结果表明立方结构的 PbS 在 309 和 373.5 nm 处出现了 2 个荧光峰, 在 211 和 232 nm 处出现了 2 个紫外吸收峰。

关键词: PbS; 多树枝; 立方结构的; 机理

中图分类号: O611.4; O613.5

文献标识码: A

文章编号: 1001-4861(2009)04-0685-08

Multiple-dendritic/Cuboidal Structured PbS: Hydrothermal Synthesis and Growth Mechanism

WANG Xin-Jun* LIU Juan CHAI Chun-Xia LI Ke DONG Yu-Tao JIANG Kai*

(College of Chemistry and Environmental Science, Henan Normal University, Xinxiang, Henan 453007)

Abstract: Well-crystalline multiple-dendritic structured lead sulfide(PbS) were prepared via a template-free, facile hydrothermal route using $\text{Pb}(\text{NO}_3)_2$ as the lead ion source, thiourea($\text{CH}_4\text{N}_2\text{S}$) as the sulfur source at 160 °C for 24 h. X-ray powder diffraction(XRD), scanning electron microscopy(SEM), energy dispersive X-ray spectroscopy(EDX) and transmission electronic microscopy(TEM) studies showed that the obtained products were face-centered cubic multiple-dendritic structured PbS with length of each dendrite from 1.0~3.0 μm . Additionally, cuboidal PbS with different concave faces was obtained through a facile hydrothermal process in an alkaline glycerol/water solution system. The edge lengths of these cuboidal microcrystals range from 2.0~5.0 μm as observed by SEM. The influencing factors for the two morphologies were discussed and the formation mechanisms were proposed based on their shape evolutions. Emission spectra of the cuboidal structure PbS was detected at 309 and 373.5 nm using a photoluminescence(PL) spectrometer, two excitonic peaks at 211 and 232 nm were observed in UV-Vis absorption spectra.

Key words: PbS; multiple-dendritic; cuboidal; mechanism

Construction of nano- or microscopic-scale inorganic materials with well-defined shape and size is an important goal of modern materials chemistry, although this still remains a key challenge^[1]. In recent years, the shape control of various nanostructures has been inten-

sively studied because of their morphology dependent properties. For example, the shape control and evolution for transition metal nanocrystals, CdSe nanocrystals, and magnetic iron oxide nanocrystals were reported by different research groups^[2-5]. As a result, those stud-

收稿日期: 2008-12-22。收修改稿日期: 2009-01-15。

国家自然科学基金(No.20571025), 河南省自然科学基金(No.0611020300)资助项目。

*通讯联系人。E-mail: wxjtg2006@126.com; Tel: 0373-3326335

第一作者: 王新军, 男, 34 岁, 博士, 副教授; 研究方向: 纳米材料的制备与表征。

ies greatly stimulate the research interests in shape and size control of nanomaterials. Size, shape, and crystal structure are crucial factors in determining the chemical, optical, and electrical properties of nanoscale materials^[6,7]. If the shape evolution processes are understood and predictable, it could be possible to program the system to fabricate materials with desired morphology and crystallinity.

The subject of inorganic dendrites has been drawing much attention since Nittmann and Stanley^[8] reported dendrites growth patterns in 1986. Many models and theories have been proposed to explain this ubiquitous phenomenon, most of them focused on nonequilibrium growth and molecular anisotropy^[9]. However, the complete understanding controllable growth of dendrites still represents a great challenge.

Lead sulfide (PbS) is a well-known IV-VI group semiconductor with a rather small bulk band gap (0.41 eV at 300 K) and a relatively large excitation Bohr radius (18 nm)^[10], which contribute to the strong quantum-confinement effect over a large nanocrystalline size range. Therefore, nanoscaled PbS has shown some novel and excellent optical and electronic properties, such as Pb²⁺-selective sensors^[11], photography^[12], and near-IR detectors^[13]. IR photodetectors, photovoltaics, electroluminescence, photoluminescence, thermal and biological images, and display devices^[14-17].

Conventionally, PbS was precipitated via the reaction between a dissoluble lead salt and H₂S gas in aqueous media. With the progress of material science, near-spherical PbS particles have been prepared in polymers, zeolites, blockcopolymer nanoreactors, inverse micelle, microemulsion and in the ethanol system through gamma-irradiation^[18-24]. Also, rectangular and rod-like PbS nanocrystals have been successfully prepared in the system containing organic polyanimes with N-chelation property such as triethylenetetramine^[25]. In 2001, Qian and coworkers^[26] reported the preparation of cubic-shaped PbS nanocrystals via a hydrothermal route under the assistance of surfactant. However, a systematic research on shape-controllable preparation of PbS in a simple aqueous solution without the assistance of any surfactant or template by hydrothermal synthesis route is

still not found in the literature. It is well known that the hydrothermal synthesis is an environmentfriendly method for preparation of materials since reactions are carried out in a sealed container. Herein, we report a facile one-step template-free hydrothermal route for the synthesis of high-quality face-centered cubic PbS at relatively low temperature (160 °C), by the reaction of easy-obtained reactants (dissoluble lead salt and thiourea). Under such conditions, toxic solvents such as ethylenediamine, pyridine and benzene can be avoided. Desired morphologies of materials have been obtained in distilled water or an alkaline glycerol/water solution without the assistance of any extra surfactant or template, and various influencing factors have been studied on the growth of PbS crystals. The formation mechanism for the multiple-dendritic and cuboidal structures PbS was discussed based on their shape evolutions. This method is favorable for green environmental protection without use of any toxicant organic solvents and surfactants.

1 Experimental

1.1 Synthesis

All of the chemical reagents used were of analytical pure grade without further purification.

For synthesis of PbS multiple-dendritic structure, a typical synthesis procedure was as follows: in the Teflon-lined stainless-steel autoclave of 50 mL capacity, 0.580 g lead nitrate (Pb(NO₃)₂) was dissolved in 45 mL deionized water under stirring, then 0.343 g thiourea (CH₄N₂S) was added 10 minutes later into the above solution under stirring for another 10 minutes. Then the Teflon-lined autoclave was sealed tightly and maintained at (130, 160, 180) °C for 24 h without shaking/stirring during the heating period and then allowed to cool to room temperature naturally. A mass of grayish-black precipitates was collected by centrifugation and washed several times with distilled water and absolute ethanol, respectively. Finally, the sample was dried in vacuum at 60 °C for 6 h.

For synthesis of PbS cuboidal structure, the starting solution was prepared by mixing 10 mL glycerol and 25 mL deionized water in the Teflon-lined stainless-steel autoclave of 50 mL capacity with a magnetic stir-

rer to form homogeneous solution. After 10 minutes stirring 0.580 g $\text{Pb}(\text{NO}_3)_2$ and 0.343 g $\text{CH}_4\text{N}_2\text{S}$ were put into the above solution in sequence under stirring for 10 min, respectively. Then 5 mL of $10 \text{ mol} \cdot \text{L}^{-1}$ NaOH solution was introduced to the above solution under stirring for another 10 min. The prepared product was similarly treated as above.

A series of experiments were carried out through changing the reaction time, reaction temperature or solvents (water, glycerol and NaOH) in order to investigate the reaction parameters influencing the morphologies of PbS microcrystals. The detailed reaction conditions and the corresponding results are shown in Table 1 and Table 2.

Table 1 Experimental conditions of multiple-dendritic structure PbS

samp	$w_{\text{Pb}(\text{NO}_3)_2} / \text{g}$	$w_{\text{CH}_4\text{N}_2\text{S}} / \text{g}$	Temperature of reactions / $^{\circ}\text{C}$	Reactions time / h	Main morphology	SEM / TEM
1	0.580	0.343	130	24	multiple-dendritic structure	Fig.3a
2	0.580	0.343	130	24	multiple-dendritic structure	Fig.3b
3	0.580	0.343	130	24	multiple-dendritic structure	Fig.3c
4	0.580	0.343	130	4	Multiple-dendritic structure and irregular cubics	Fig.3d
5	0.580	0.343	160	48	cuboidal structure	Fig.3e
6	0.580	0.343	180	48	cuboidal structure	Fig.3f

Table 2 Experimental conditions of cuboidal structure PbS

Sample	$w_{\text{Pb}(\text{NO}_3)_2} / \text{g}$	$w_{\text{CH}_4\text{N}_2\text{S}} / \text{g}$	Glycerol / mL	Temperature of reactions / $^{\circ}\text{C}$	Reaction time / h	$10 \text{ mol} \cdot \text{L}^{-1}$ NaOH / mL	Main morphology	SEM
1	0.580	0.343	10	130	24	5	cuboidal structure with different concave faces	Fig.4a
2	0.580	0.343	10	130	32	5	cuboidal structure with different concave faces	Fig.4b
3	0.580	0.343	10	130	48	5	cuboidal structure with different concave faces	Fig.4c
4	0.580	0.343	10	160	24	0	semi-microflowers	Fig.4d
5	0.580	0.343	10	180	24	0	microflowers	Fig.4e

1.2 Characterization

The as-prepared samples were characterized by XRD, SEM, EDX and TEM, respectively. The phase purity of the as-synthesized products were examined by XRD using a Bruker advance-D8 X-ray powder diffractometer (40 kV, 100 mA) equipped with graphite monochromatized $\text{Cu } K\alpha$ radiation ($\lambda = 0.154 \text{ nm}$). The scan rate of $0.06^{\circ} \cdot \text{s}^{-1}$ was applied and the patterns was recorded in the 2θ range of $10^{\circ} \sim 80^{\circ}$. The morphology of the prepared products were observed on a scanning electron microanalyzer (JSM-6390LV, 30 kV). EDX was carried out on a Hitachi S-4700 equipped with energy dispersive X-ray Spectrometer. The TEM studies were carried out on a JEM-100SX (Japan) apparatus with accelerating voltage of 200 kV. UV-Vis absorption spectra were recorded on a Hitachi U-4100

spectrophotometer with the samples dispersed in alcohol at room temperature. Photoluminescence (PL) spectra were taken in a Hitachi 850-fluorescence spectrophotometer with a xenon lamp at room temperature. The excitation wavelength was 260 nm. The samples for TEM observation were dispersed in absolute ethanol with ultrasonic vibration for 1 h, and one drop of solution was dropped onto the surface of copper grids before evaporating naturally. The solution used in UV-Vis experiment was obtained by dispersing 10 mg PbS products in 100 mL ethanol.

2 Results and discussion

2.1 XRD, EDX results

The typical XRD patterns of the obtained sample are shown in Fig.1, which were synthesized at 160°C

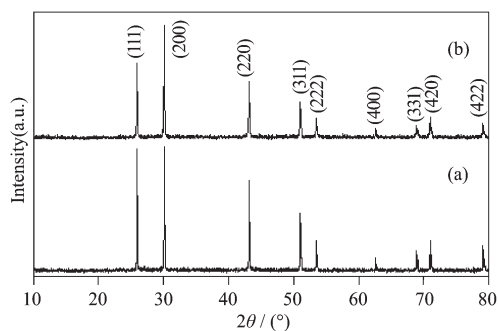


Fig.1 XRD patterns of (a) multiple-dendritic and (b) cubodical structured PbS at 160 °C for 24 h

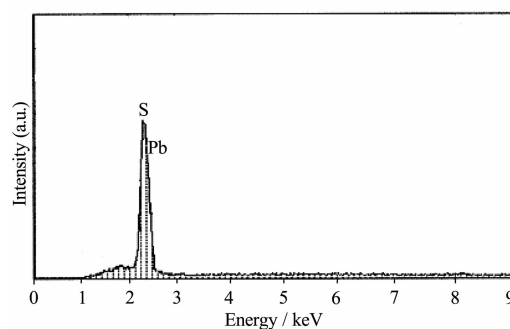


Fig.2 EDX spectrum of the cubodical structure PbS at 160 °C for 24 h

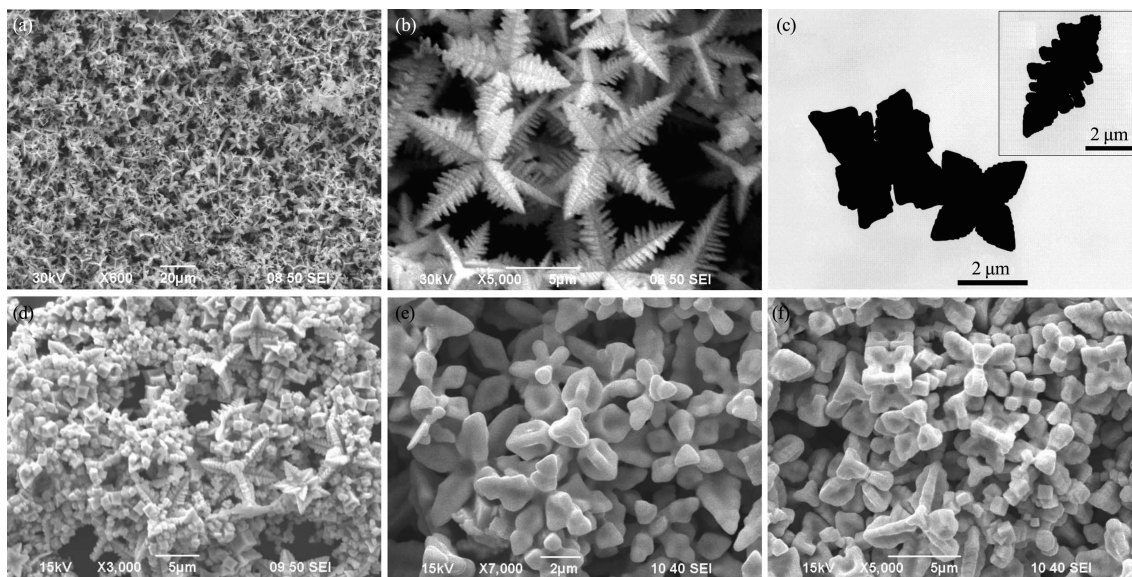
for 24 h in water and an alkaline glycerol/water solution, respectively(Fig.1a and Fig.1b). All the diffraction peaks can be readily indexed as the face-centered cubic (fcc) structure PbS with lattice constant of $a=0.594$ nm, which is agreement with the literature datum($a=0.593$ 6 nm(PDF No.05-592))^[27]. No impurity such as Pb or PbO is detected in the pattern. The strong and sharp peaks indicate that the samples are well crystallized.

The cubodical structured PbS was also analyzed by EDX, and the result is shown in Fig.2. According to the EDX spectra, the chemical components of the sample are Pb and S. The weight percentages of Pb and S are 88.87% and 11.13%, respectively. Quantification of the EDX peaks shows that the molar ratio of Pb to S is 1.1:1, close to the stoichiometry of PbS.

Because the ionization energy of Pb and S is very close, in the EDX spectra the positions of Pb and S are overlapped.

2.2 SEM, TEM results for multiple-dendritic structure PbS

Fig.3 are typical SEM images of the PbS microcrystals in different reaction conditions. Fig.3a(sample 1) shows a SEM image at low magnification of the as-prepared PbS multiple-dendrites synthesized in distilled water at 130 °C for 24 h. As shown in the panoramic image Fig.3a(sample 1), the synthesized PbS by this method is uniform in size. Fig.3b(sample 2) shows a SEM image at higher magnification of the as-prepared PbS, close observations in Fig.3b(sample 2) reveal a well defined multiple-dendritic structure with



(a) the panoramic image; (b) the enlarged image; (c) TEM images of the multiple-dendrites and individual dendritic; SEM images of multiple-dendritic structure PbS at (d) 130 °C for 4 h, (e) 160 °C for 48 h, (f) 180 °C for 48 h

Fig.3 SEM images of the multiple-dendritic structure PbS at 130 °C for 24 h

four pronounced dendritic-shaped offshoots distributing symmetrically in each side. A typical TEM image is shown in Fig.3c(sample 3), indicating that the multiple-dendritic structure PbS are with 4-fold structural symmetry and each dendritic offshoot has 3D structure consisting of one trunk and small branches. The size of multiple-dendritic structure PbS is calculated to be approximately 2.5 μm .

Fig.3d(sample 4) is the SEM image of the obtained sample at 130 $^{\circ}\text{C}$ for 4 h. It is clearly seen that the products are poor crystalline PbS multiple-dendritic structures coexisting with lots of irregular cubics. When the reaction time is 24 h, well crystalline PbS with sharp multiple-dendritic structure is obtained as shown in Fig. 3b(sample 2). While at higher reaction temperatures, such as 160 and 180 $^{\circ}\text{C}$, the dendritic-shaped offshoots gradually disappear, leaving cuboidal only, as shown in Fig.3e(sample 5) and 3f(sample 6).

2.3 SEM results for cuboidal structure PbS and effect factors

Figs.4a~c(sample1~3) show the SEM images of the sample obtained in an alkaline glycerol/water solution system at 130 $^{\circ}\text{C}$ with different durations. In glycerol (10 mL)-H₂O (25 mL) solvent cuboidal structure PbS is obtained. From Figs.4a-c (sample1-3) some interesting phenomena can be observed: firstly, some cuboidals in the sample have a concavity on each of their faces; secondly, the concavity becomes larger and larger with the duration time. Many cuboidals with edge lengths from 2.0 to 5.0 μm are present in the sample, and the proportion of the cuboidal in the sample is estimated to be 60%. By comparison with multiple-dendritic structure PbS, upon the addition of glycerol and NaOH, the morphologies of the products are changed greatly, indicating the great effect of glycerol and NaOH in the reaction system on the morphologies of the PbS.

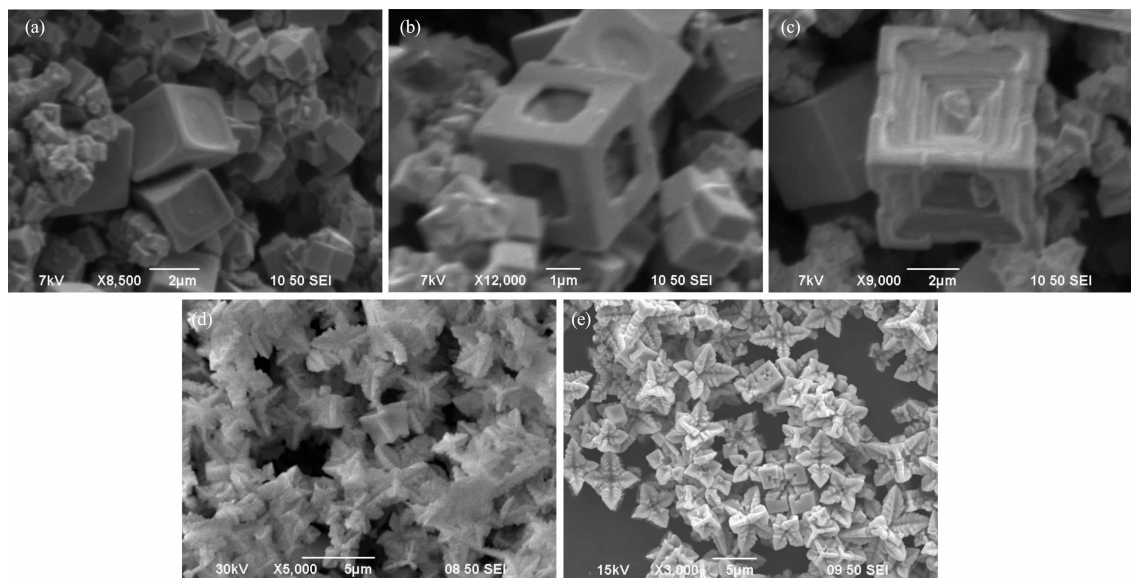


Fig.4 SEM images of the cuboidal structure PbS at 130 $^{\circ}\text{C}$ with different durations (a) 24 h; (b) 32 h; (c) 48 h and SEM images of PbS without NaOH at (d) 160 $^{\circ}\text{C}$ for 24 h,(e) 180 $^{\circ}\text{C}$ for 24 h

As for cuboidal structure PbS, in addition to reaction temperature and time, NaOH alkaline solution also has an overt influence on the finally cuboidal structure. Fig.4d,e(sample 4,5) show the SEM image of the obtained sample at 160(180) $^{\circ}\text{C}$ for 24 h without the addition of NaOH, which shows no cuboidal structure with different concave faces. Instead we observe a continuous transformation of morphologies from cuboidal to se-

mi-microflowers and finally to microflowers with increasing synthesis temperature and reaction time. These might have relation to the glycerol and NaOH. In our work, glycerol acts as a complexing reagent to form the complex, $\text{Pb}(\text{C}_3\text{H}_6\text{O}_3)_2$, which sharply decreases the free Pb^{2+} concentration in the solution and slows down the speed of the following reaction for the formation of PbS crystals, NaOH provides an alkaline environment for

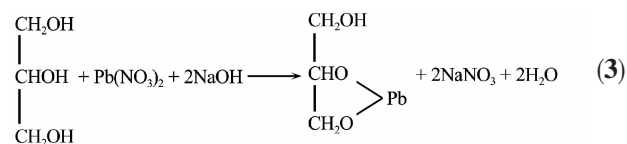
the $\text{Pb}(\text{C}_3\text{H}_6\text{O}_3)$, and this alkaline environment is favorable for the cuboidal structure formation.

2.4 Formation mechanism

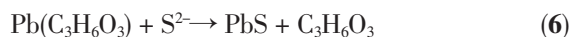
In the approach to construct multiple-dendritic structure, the formation of PbS is based on the combination of Pb^{2+} and S^{2-} . While in the case of NO_3^- , only S^{2-} coordinates with Pb^{2+} , which might favor the quicker growth of the $\langle 111 \rangle$ faces. This phenomenon can be attributed to the different interaction between anions and Pb^{2+} . During the growth process, the adsorption rate of S^{2-} on different planes of PbS nuclei may be affected by the anions. The formation of PbS structures involves the formation and growth processes of PbS nuclei. It is well known that thiourea can decompose at certain temperature to produce H_2S . And the reaction of H_2S and Pb^{2+} occurs to produce PbS nuclei. The possible chemical process for the formation of PbS can be summarized as follows:



In the alkaline glycerol/water solution system, glycerol acts as a complexing reagent to form the complex, $\text{Pb}(\text{C}_3\text{H}_6\text{O}_3)$; NaOH provides an alkaline environment for the $\text{Pb}(\text{C}_3\text{H}_6\text{O}_3)$, which sharply decreases the free Pb^{2+} concentration in the solution and slows down the speed of the following reaction for the formation of PbS crystals. The whole reaction process can be summarized as follows:



Slow reaction rate is favorable for crystallization as well as for the separation of the growth step and the nucleation step.



On the basis of our experiments, we assume the growth process of the two kinds of PbS structures to be a nucleation-preferential growth process. It was concluded by Murphy^[28] that the preferential absorption of molecules and ions in solution to different crystal faces

directs the growth of nanoparticles into various shapes by controlling the growth rate along different crystal axes. For the face-center-cubic(fcc) nanocrystal, Wang^[29] suggested that the shape was mainly determined by the ratio of the growth rate in the $\langle 100 \rangle$ to that in the $\langle 111 \rangle$, and cuboidal bound by the six $\langle 100 \rangle$ planes would be formed when the ratio was relatively lower. Cheon and co-workers^[30] verified the above conclusion. They found that the faster growth on the $\langle 111 \rangle$ faces favored the formation of cube-shaped PbS crystals. Recently, Qian et al^[31] further confirmed the above conclusion during their work on the shape evolution of fcc Cu_2O crystals. They observed the shape evolution of Cu_2O crystals from eight pod particles through star-shaped particles to cubes. Then, with respect to the structure of fcc PbS, we speculate that these structures are formed in an analogous process. In our experiments, we observed the shape evolution of PbS crystals on the basis of the XRD and SEM analyses. As illuminated by the XRD (Fig.1), the $\langle 111 \rangle$ 、 $\langle 200 \rangle$ and $\langle 220 \rangle$ reflections are relatively strong compared with the standard stick pattern for bulk PbS, indicating that the obtained PbS have a preferential growing facet. At the initial stage, because of the production of PbS, the supersaturation of the system rapidly increases and the produced PbS gradually nucleates and grows. Because of the faster growth on the $\langle 111 \rangle$ faces, the cuboid products are obtained(sample 4), as shown in Fig.3d. Then, the adsorption and desorption of the excess thiourea ions on the different planes of cuboid PbS particles may kinetically favor the preferential crystal growth along eight $\langle 111 \rangle$ directions. As a result, continuous growth of PbS in the $\langle 111 \rangle$ direction, the multiple-dendritic structure is obtained(sample 1,2), as shown in Fig. 3a,b. For the cuboidal structure PbS, glycerol acts as a complexing reagent to form the complex $\text{Pb}(\text{C}_3\text{H}_6\text{O}_3)$ in alkaline solution shown in Eq. (3), which proceeds more slowly compared with that in Eq.(1,2). The lower concentration of Pb^{2+} in the reaction system leads to the slower growth of the PbS crystal. The slow growing rate is favorable for the formation of thermodynamically stable structure, and, thus, for PbS unit, the cuboidal is the thermodynamically stable morphology. However,

on the other hand, the initial growth preferentially along $\langle 111 \rangle$ due to the presence of glycerol gives birth to some incomplete $\langle 100 \rangle$ faces in the cuboidal. Consequently, integrative contribution of the preferential growth along $\langle 111 \rangle$ due to the glycerol followed by the thermodynamically stable growth of $\langle 100 \rangle$ faces causes slower growing rate, cuboidal structures are obtained in such a reaction system (sample 1~3), as shown in Fig. 4a~c.

2.5 Optical properties of cuboidal structure PbS

Fig.5 shows the UV-Vis absorption spectrum of PbS nanoparticles. The absorption peaks at 211 and 232 nm are observed in the spectrum. Our results are in good agreement with literature reports. The threshold of the absorption is obvious blue shifted compared with the bulk PbS^[32,33], presumably attributing to the quantum-confinement effect of PbS. Most research groups reported a broad featureless absorption band with absorption offset position varying in general between 500 and 1100 nm.

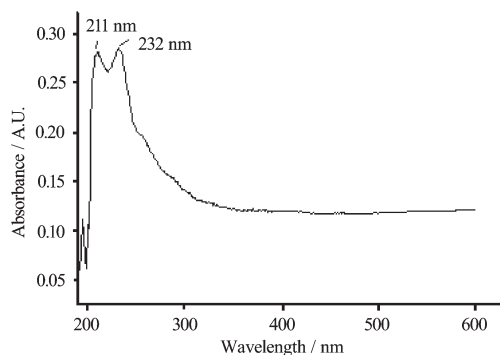


Fig.5 UV-Vis spectrum of the products dispersed in ethanol

The PL spectrum of PbS is shown in Fig.6. Two sharp PL peaks, indicating the product with narrow size distribution, centered at 309 and 373.5 nm, are observed in the PL spectra of nanocrystalline PbS. Com-

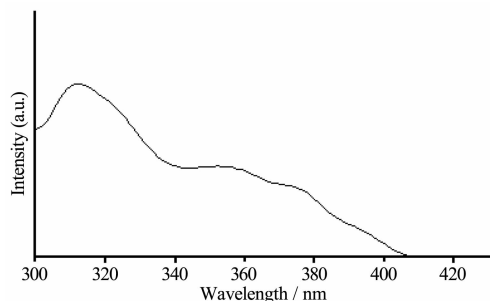


Fig.6 PL spectrum of the product which is dispersed in ethanol at the room-temperature

pared with its bulk counterpart, the PL spectrum of the as-prepared PbS shows a broadened peak due to the small dimension of the nanoparticles in their wall, exhibiting a blue shift in the PL spectrum^[34]. These have resulted from strong quantum confinement effect, indicating the quantum size effect on nanocrystalline PbS.

3 Conclusions

In summary, multiple-dendritic and cuboidal structures PbS have been synthesized through an one-step template-free hydrothermal method. XRD, SEM, EDX, and TEM results indicate that the obtained samples are pure face-center-cubic (fcc). Starting materials, reaction temperature and reaction time play the key role in the morphology of the final products. Additionally, glycerol and NaOH alkaline solution play an important role in the cuboidal structure PbS. Based on the experimental results, formation mechanisms for the two structures PbS are proposed. The optical properties of the cuboidal structure PbS differ from those of the bulk crystals, which could be related to their structural complexity. Work for properties of the PbS nanocrystals is in progress.

References:

- [1] (a) Hu J, Odom T W, Lieber C M. *Acc. Chem. Res.*, **1999**, *32*: 435~445
 (b) Xia Y, Yang P, Sun Y, et al. *Adv. Mater.*, **2003**, *15*: 353~389
- [2] Petroski J M, Wang Z L, El-Sayed M J. *Phys. Chem. B*, **1998**, *102*: 3316~3320
- [3] Bradley J S, Tesche B, Busser W, et al. *J. Am. Chem. Soc.*, **2000**, *122*: 4631~4636
- [4] Peng Z A, Peng X G. *J. Am. Chem. Soc.*, **2001**, *123*: 1389~1395
- [5] Cheon J C, Kang N J, Lee S M, et al. *J. Am. Chem. Soc.*, **2004**, *126*: 1950~1951
- [6] Ding Z F, Quinn B M, Haram S K, et al. *Science*, **2002**, *296*: 1293~1297
- [7] Alivisatos A P. *Science*, **1996**, *271*: 933~937
- [8] Nittmann J, Stanley H E. *Nature*, **1986**, *321*: 663~668
- [9] (a) Langer J S. *Rev. Mod. Phys.*, **1980**, *52*: 1~28
 (b) Libbrecht K G, Tanusheva V M. *Phys. Rev. Lett.*, **1998**, *81*: 176~179
 (c) Karma A, Rappel W J. *Phys. Rev. Lett.*, **1996**, *77*: 4050~4053
 (d) Chait A, Pines V, Zlatkowski M. *J. Crystal Growth*, **1996**,

- 167:383~386
- (e) Ben-Jacob E, Garik P. *Nature*, **1990**,**343**:523~530
- (f) Xiong Y, Xie Y, Du G, et al. *J. Solid State Chem.*, **2002**,**166**:336~340
- (g) Hollander F F A, Stasse O, Suchtelen J van, et al. *J. Crystal Growth*, **2001**,**233**:868~880
- [10] Machol J L, Wise F W, Patel R C, et al. *Phys. Rev. B*, **1993**,**48**:2819~2822
- [11] Hirata H, Higashiyama K. *Bull. Chem. Soc. Jpn.*, **1971**,**44**:2420~2423
- [12] Nair P K, Gomezdaza O, Nair M T S. *Adv. Mater. Opt. Electron*, **1992**,**1**:139~145
- [13] Gadenne P, Yagil Y, Deutscher G. *J. Appl. Phys.*, **1989**,**66**:3019~3025
- [14] Zhang Z H, Lee S H, Vittal J J, et al. *Phys. Chem. B*, **2006**,**110**:6649~6654
- [15] Zhang H, Zuo M, Tan S, et al. *Nanotechnology*, **2006**,**17**:2931~2936
- [16] Zhao N N, Qi L M. *Adv. Mater.*, **2006**,**18**:359~362
- [17] Xu L Q, Zhang W Q, Ding Y W, et al. *J. Cryst. Growth*, **2004**,**273**:213~219
- [18] Wang Y, Suna A, Mahler W, et al. *J. Chem. Phys.*, **1987**,**87**:7315~7322
- [19] Wang S, Yang S. *Langmuir*, **2000**,**16**:389~397
- [20] Wang Y, Herron N. *J. Phys. Chem.*, **1987**,**91**:257~260
- [21] Kane R S, Cohen R E, Silbey R. *Chem. Mater.*, **1996**,**8**:1919~1924
- [22] Liveri V T, Rossi M D, Arrigo G, et al. *Appl. Phys. A*. **1999**,**69**:369~373
- [23] Yang J P, Qadri S B, Ratna B R. *J. Phys. Chem.*, **1996**,**100**:17255~17259
- [24] Qiao Z, Xie Y, Xu J, et al. *J. Colloid Interface Sci.* **1999**,**214**:459~461
- [25] Sugimoto T, Chen S H, Muramatsu A. *Colloids Surf. A*. **1998**,**135**:207~226
- [26] Jiang Y, Wu Y, Xie B, et al. *J. Cryst. Growth*, **2001**,**231**:248~251
- [27] *Powder Diffract. File, JCPDS Int. Centre Diffract. Data*, **2001**, 19073~3273, USA.
- [28] Murphy C J. *Science*, **2002**,**298**:2139~2141
- [29] Wang Z L. *J. Phys. Chem. B*, **2000**,**104**:1153~1175
- [30] Lee S M, Cho S N, Cheon J W. *J. Adv. Mater.*, **2003**,**15**:441~444
- [31] Wang D, Mo M, Yu D, et al. *Cryst. Growth Des.*, **2003**,**3**:717~720
- [32] Wang Y, Suna A, Mahler W, et al. *J. Chem. Phys.*, **1987**,**87**:7315~7322
- [33] Zhao N N, Qi L M. *Adv. Mater.*, **2006**,**18**:359~362
- [34] Yang P, Song C F, Lu M K, et al. *Chem. Phys. Lett.*, **2001**,**345**:429~434